Phasic excitation of dopamine neurons in ventral VTA by noxious stimuli

Frédéric Brischoux[1], Subhojit Chakraborty[1], Daniel I. Brierley, and Mark A. Ungless[2]

Medical Research Council Clinical Sciences Centre, Imperial College London, Hammersmith Hospital, Du Cane Road, London W12 0NN, United Kingdom

Edited by Ann M. Graybiel, Massachusetts Institute of Technology, Cambridge, MA, and approved January 15, 2009 (received for review November 12, 2008)

Midbrain dopamine neurons play central roles in reward processing. It is widely assumed that all dopamine neurons encode the same information. Some evidence, however, suggests functional differences between subgroups of dopamine neurons, particularly with respect to processing nonrewarding, aversive stimuli. To directly test this possibility, we recorded from and juxtacellularly labeled individual ventral tegmental area (VTA) dopamine neurons in anesthetized rats so that we could link precise anatomical position and neurochemical identity with coding for noxious stimuli. Here, we show that dopamine neurons in the dorsal VTA are inhibited by noxious footshocks, consistent with their role in reward processing. In contrast, we find that dopamine neurons in the ventral VTA are phasically excited by footshocks. This observation can explain a number of previously confusing findings that suggested a role for dopamine in processing both rewarding and aversive events. Taken together, our results indicate that there are 2 functionally and anatomically distinct VTA dopamine systems.

aversive | midbrain | reward | salient | stress

Midbrain dopamine neurons of the ventral tegmental area (VTA) and substantia nigra pars compacta (SNc) play key roles in reward processing (1, 2). Although dopamine neurons exhibit considerable heterogeneity regarding projection targets and basic pharmacological properties (3–5), it is widely assumed that they exhibit homogenous reward coding across the entire population (1). In addition, we have reported that dopamine neurons are uniformly inhibited by aversive stimuli, which is consistent with reward theories; a separate group of VTA neurons that are excited by noxious stimuli are not dopaminergic (6). However, there are a number of findings that are difficult to reconcile with this view. First, aversive stimuli evoke dopamine release at projection targets, as measured with microdialysis, particularly in the medial shell of the nucleus accumbens (mAcSh) and the medial prefrontal cortex (7, 8). Second, dopamine appears to play an important role in fear conditioning (9). For example, dopamine receptor antagonists block fearful behavior when infused into mAcSh (10). Detailed anatomical work has shown a strong, reciprocal connection between ventromedial VTA and the mAcSh, suggesting a closed-loop circuit, in contrast to the feed-forward loops proposed for the rest of the mesostriatal system (11–13). We noted that many electrophysiological studies target the dorsorostral VTA, predominantly the large parabrachial pigmented nucleus (PBP). It is possible, therefore, that ventromedial dopamine neurons [particularly the paranigral nucleus (PN)] have been relatively neglected by previous studies, and we hypothesized that these neurons might be excited by noxious stimuli. To directly test this, we recorded from and labeled individual neurons in both dorsal and ventral VTA in anesthetized rats so that we could deliver temporally controlled, intense noxious stimulus (electric shock to the hind paw) and determine the precise anatomical location and neurochemical identity of individual neurons (14). In this study we refer to the footshock as noxious because it was intense enough to activate nociceptors associated with actual or potential tissue damage (15). In the awake, freely moving animal, this stimulus would be aversive and could act as a punisher.

Results

Electrophysiological Characteristics of Neurochemically Identified VTA Neurons. We recorded extracellular activity from single VTA neurons and delivered multiple (20 Hz), intense (5 mA), and prolonged trains (4 s) of electric shocks to the hind paw. Following this, the individual recorded neurons were labeled with Neurobiotin by using the juxtacellular technique (14). This allowed us to precisely map the location of the neuron postmortem by using established cytoarchitectonic features (11, 16) and to neurochemically identify it with immunofluorescence for tyrosine hydroxylase (TH; the rate-limiting enzyme for dopamine synthesis). Based on our previous work, we deliberately searched for VTA neurons with relatively broad action potentials (APs) in an attempt to avoid the population of nondopaminergic neurons that have similar electrophysiological properties to dopamine neurons (but with narrower APs) (6). However, as expected, we still found some nondopaminergic neurons within our sample ($n = 4$), which emphasizes the importance of confirming neurochemical identity through single-cell labeling and immunohistochemistry. It has been suggested that using a high-pass filter setting of 50 Hz is important for distinguishing between dopaminergic and nondopaminergic VTA neurons on the basis of their AP waveform (17). We have now directly tested this and find, in fact, that this does not help in electrophysiologically distinguishing VTA neurons. Under these conditions (i.e., 50-Hz high-pass filter), dopamine neurons ($n = 14$) and nondopamine neurons ($n = 4$) exhibited similarly shaped biphasic APs of the same duration [from start to trough (mean ± SEM): dopamine neurons 1.62 ± 0.08 ms vs. nondopamine neurons 1.75 ± 0.41 ms, $P = 0.62$, t test]. The neurochemical identity of these nondopaminergic neurons is currently unknown, but it is unlikely that they are γ-aminobutyric acid (GABA)-ergic, because identified GABAergic neurons in the VTA have different electrophysiological characteristics [i.e., very rapid APs (full duration <1.5 ms) and high firing rates (>10 Hz)] (18, 19). We and others have described a discrete population of putatively glutamatergic neurons concentrated in the rostral VTA, which may represent these TH-negative neurons (20, 21).

Phasic Responses of VTA Dopamine Neurons to Noxious Stimuli. Consistent with our previous work, in the majority of putative dopamine neurons we observed a rapid inhibition or no significant response to the noxious footshocks. We successfully labeled 9 of these neurons (5 inhibited; 4 unresponsive) that were TH-positive (Fig. 1 *A–C*). These neurons were located primarily in the dorsal part of the VTA (Fig. 1*G*). In addition, we labeled 5 TH-positive neurons that were strongly excited by the foot-

Author contributions: F.B., S.C., and M.A.U. designed research; F.B., S.C., and D.I.B. performed research; F.B., S.C., and M.A.U. analyzed data; and F.B., S.C., D.I.B., and M.A.U. wrote the paper.

The authors declare no conflict of interest.

This article is a PNAS Direct Submission.

[1]F.B. and S.C. contributed equally to this work.

[2]To whom correspondence should be addressed. E-mail: mark.ungless@imperial.ac.uk.

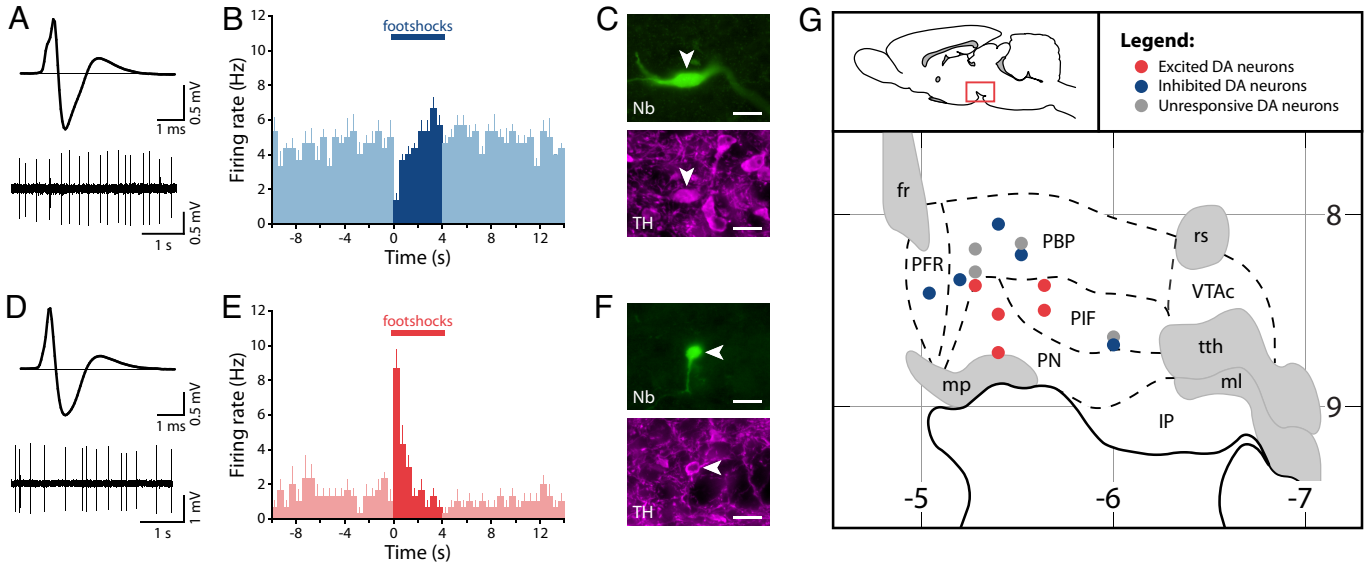

Fig. 1. Dorsal VTA dopamine neurons are inhibited by noxious stimuli, whereas ventral VTA dopamine neurons are excited. (*A*) Averaged extracellular waveform and baseline firing activity from a recorded neuron. (*B* and *C*) This neuron (*B*) showed an inhibitory response to footshocks (peristimulus time histogram averaged across 6 footshocks; mean + SEM; 500-ms bins) and was (*C*) immunohistochemically identified as dopaminergic (Nb indicates Neurobiotin). (*D–F*) In contrast, a second neuron with a similar averaged extracellular waveform and baseline firing rate (*D*) showed an excitatory response to footshocks (*E*), but was also immunohistochemically identified as dopaminergic (*F*). (Scale bars: 20 μm.) (*G*) A parasagittal schematic view of the VTA (lateral, 0.6 mm) showing the distribution of individual dopamine neurons and their responses to footshocks and showing a clear anatomical segregation of functional subgroups (horizontal numbers are distance from bregma in millimeters; vertical numbers are depth in millimeters). fr indicates fasciculus retroflexus; IP, interpeduncular nucleus; ml, medial lemniscus; mp, mammillary peduncle; PBP, parabrachial pigmented nucleus; PFR, parafasciculus retroflexus area; PIF, parainterfascicular nucleus; PN, paranigral nucleus; rs, rubrospinal tract; tth, trigeminothalamic tract; and VTAc, ventral tegmental area caudal.

shocks (Fig. 1 *D–F*). Strikingly, these neurons were located in the ventral part of the VTA in, or close to, the PN (Fig. 1*G*). It was, typically, harder to find and juxtacellularly label excited dopamine neurons compared with inhibited dopamine neurons, which may be one reason many previous studies could have overlooked this population. Their firing rates and AP waveform characteristics were similar to those of inhibited dopamine neurons [mean ± SEM: excited dopamine neurons ($n = 5$): firing rate, 2.68 ± 0.58 Hz; AP width (start to trough), 1.25 ± 0.15 ms vs. inhibited dopamine neurons ($n = 5$): firing rate, 3.70 ± 0.67 Hz; AP width, 1.09 ± 0.11 ms; $P = 0.28$ and $P = 0.43$, respectively, t test; Fig. 1 *A* and *D*]. The phasic excitation peaked around 150 ms after the onset of the footshock (Fig. 2), which is similar to the latency of the well-described rapid excitation seen in most putative dopamine neurons in response to unexpected rewards (1). It is not clear which region is driving this rapid response, but one possibility is the lateral habenula, which has been implicated as the source of negative reward prediction errors in dopamine neurons (22).

Firing Patterns of VTA Dopamine Neuron Subgroups. Midbrain dopamine neurons can fire in single-spike or bursting mode. Bursts are typically defined as starting with an interspike interval (ISI) of < 80 ms and finishing with an ISI > 160 ms (23). Bursts play an important role in dopamine signaling, because at higher frequencies, such as those that occur in a burst, it is thought that the dopamine transporter becomes overwhelmed and extracellular dopamine increases supralinearly (24). We found that dopamine neurons in the ventral VTA that were excited by the footshocks had particularly high levels of bursting compared with dopamine neurons in the dorsal VTA that were inhibited by the footshocks [mean % of spikes in burst ± SEM: excited ($n = 5$), 28.71 ± 10.47; inhibited ($n = 5$), 2.58 ± 1.18; $P = 0.016$; Mann–Whitney U test; Fig. 3 *A–C*]. Dopamine neurons that were excited by the footshocks also had a higher coefficient of variation (CV; a measure of regularity) of their ISIs compared with dopamine neurons that were inhibited by the footshocks [mean ± SEM: excited ($n = 5$), 0.81 ± 0.14; inhibited ($n = 5$), 0.35 ± 0.57; $P = 0.028$; Mann–Whitney U test]. Given this relationship between anatomical position and burst firing, it is tempting to speculate that it may be related to different synaptic inputs, although it could also involve differences in their intrinsic excitability (e.g., differential expression of ion channels) (25). Interestingly, nondopamine neurons had relatively low levels of bursting and ISI CVs (Fig. 3*C*), which suggests that by combining responsivity to footshocks with burst/regularity analysis, it is possible to get a good indication of neurochemical identity and location of the recorded neuron. It is often assumed that

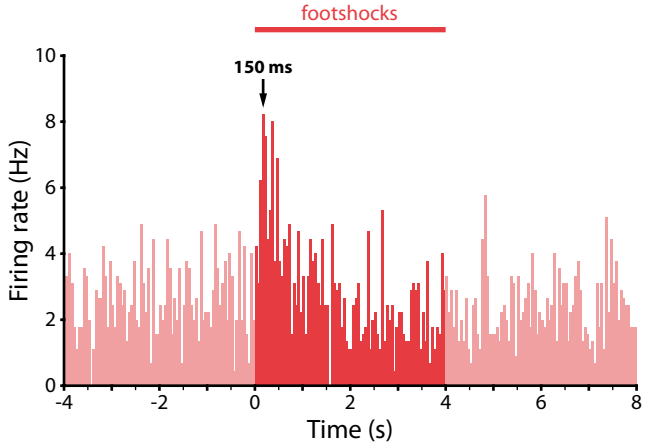

Fig. 2. Footshock-evoked excitations in ventral VTA dopamine neurons have a rapid onset, similar to that seen for reward-related excitations in dopamine neurons in previous studies. Population peristimulus time histogram for the 5 identified dopamine neurons that exhibited an excitatory response to footshocks (50-ms bins).

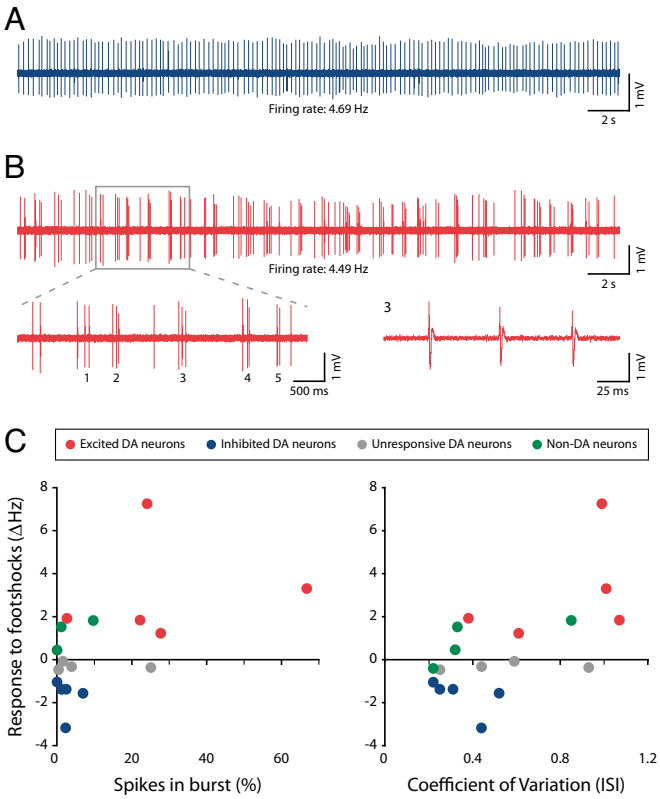

Fig. 3. Dopamine neurons that are inhibited by the noxious stimulus show tonic, low-bursting, single-spike activity, whereas dopamine neurons that are excited by the noxious stimulus show high levels of bursting. (*A*) Tonic firing activity in an identified dopamine neuron that was inhibited by the footshocks. (*B*) Bursting activity in an identified dopamine neuron that was excited by the footshocks (*Upper*). (*Lower*) An expanded view of 5 bursts (*Left*) and the third burst (*Right*). (*C*) Scatter plots showing change in response to footshock as a function of the percentage of spikes in burst (*Left*) or CV of the ISI (*Right*). Dopamine neurons that were excited by the footshocks had higher levels of bursting and higher ISI CVs than either dopamine neurons that were inhibited by the footshocks or nondopamine neurons [1 nondopamine neuron could not be analyzed for bursts because its high-baseline firing rate (9.14 Hz) meant that its mean ISI fell within the burst criteria].

dopamine neurons can change between tonic and burst firing states. Our results suggest the interesting possibility that dopamine neurons, depending on their location in the VTA, may be more or less likely to be in 1 of these 2 states.

Phasic Excitation of Dopamine Neurons at the Termination of Noxious Stimulation. Behavioral experiments show that the termination of an aversive stimulus can act as a reward (26), and therefore might be expected to excite dopamine neurons (27). Previous studies have reported synchronization of firing following termination of a noxious stimulus in SNc (28), but do not report an increase in firing rate in either SNc or VTA dopamine neurons (6, 28). However, stimuli used previously were either extremely brief or not particularly intense. In contrast, we delivered a stimulus that was both intense and prolonged and found that many dorsal dopamine neurons were clearly excited during the first 500 ms following the termination of the footshocks (as exemplified in Fig. 4 *A–C*). Of the 9 neurochemically identified dopamine neurons that were initially inhibited or unresponsive at the onset of the footshocks, 5 showed a significant, phasic excitation at the termination of the footshocks (Fig. 4*D*). This phasic excitation peaked between 100 and 150 ms after the termination of the footshocks (Fig. 4*E*). This excitation at stimulus offset may contribute to the dopamine release seen in response to aversive stimuli, as measured by using microdialysis. However, it is unlikely to be solely responsible, because the increased dopamine release is often large and can occur during stimulus presentation (29). Importantly, this observation can help explain why dopamine receptor antagonists interfere with avoidance learning, where the rewarding role of the offset of an aversive stimulus drives behavior (30).

Discussion

Considerable attention and controversy have been focused on 2 types of theory of information coding in dopamine neurons (31–33). One states that dopamine neurons are selectively excited by unexpected rewards and reward-predicting stimuli (1); the other states that dopamine neurons are activated by all salient stimuli (33). Our results suggest a novel resolution to this controversy, which is that these 2 types of theory refer to 2 functionally and anatomically distinct VTA dopamine systems. It is well known that subgroups of VTA dopamine neurons have different projection targets (11), and it seems likely that this will relate to the functionally distinct populations recorded here. However, the targets for the neurons in this study are unknown, and an important next step will be to directly link the neuronal populations recorded here to these different projection systems. We believe that previous studies have predominantly characterized dorsal VTA dopamine neurons, which are selectively activated by rewards (1) and inhibited by noxious stimuli (6). In contrast, we now show that ventral VTA dopamine neurons are excited by noxious stimuli, which suggests the possibility that they may encode saliency. A key test of this proposal will be to investigate how these ventral dopamine neurons respond to rewards.

Our findings can help explain a number of observations that have been particularly problematic for single-system reward theories. For example, aversive stimuli evoke dopamine release at projection targets (7, 8), particularly those that receive strong innervation from the PN (i.e., the medial prefrontal cortex and the shell of the nucleus accumbens). This point remains somewhat speculative, because the projection targets of our excited neurons are currently unknown. Another troublesome finding has been that dopamine receptor antagonists interfere with the acquisition and expression of aversive conditioning (9). Our results suggest that in both of these cases activation of ventral VTA dopamine neurons may be involved. Moreover, recent studies have highlighted functional differences between rostral and caudal VTA (34–38). For example, overexpression of glutamate receptor subunit 1 or cAMP response element-binding protein in the rostral parts of the VTA causes conditioned place preference to morphine, but in caudal VTA this leads to conditioned place aversion (34, 38). In addition, overexpression of phospholipase Cγ in caudal VTA enhances responsiveness to nociceptive stimuli (35). It is possible that these studies differentially targeted the inhibited and excited dopamine neuron populations described here. The caudal VTA in these studies refers to a region that comprises both the PBP and the compact PN (Fig. 1*G*) (11). In contrast, the rostral VTA comprises the rostral part of the PBP and the parafasciculus retroflexus (Fig. 1*G*) (11).

Last, it will be important to directly compare dorsal and ventral VTA dopamine neuron activity in freely moving, awake animals. Although it is not currently feasible to use the juxtacellular labeling technique in freely moving animals, careful single-neuron recordings that systematically explore the entire VTA may still be informative. In any case, it is likely that our findings can be extrapolated to awake animals because dopamine neuron properties and responses to noxious events appear to be relatively unaffected by anesthesia (39–42).

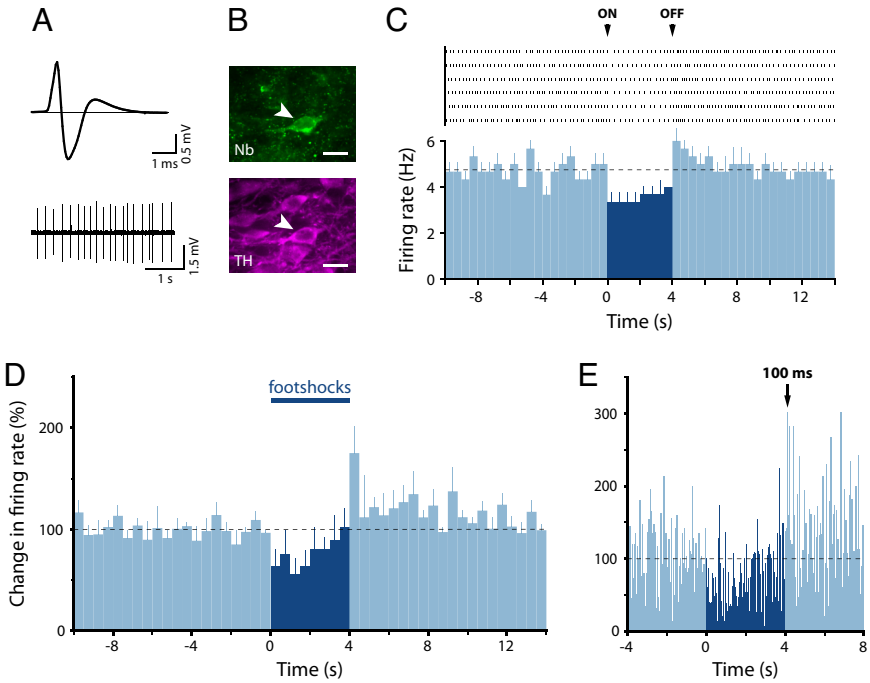

Fig. 4. Many dopamine neurons that are inhibited by (or unresponsive to) the footshocks show a significant excitation at the termination of the stimulus. (*A*) Averaged extracellular waveform and baseline firing activity from a recorded neuron. (*B*) The same neuron was immunohistochemically identified as dopaminergic (Nb indicates Neurobiotin). (Scale bars: 20 μm.) (*C*) A cumulative raster plot of this neuron (*Upper*) and the resulting peristimulus time histogram (*Lower*) averaged across 6 footshocks (mean + SEM; 500-ms bins) showed an inhibitory response following the onset (ON) of the stimulation and an excitation following its offset (OFF). Black dashed line indicates mean baseline firing rate. (*D*) Population peristimulus time histograms (500-ms bins; mean + SEM) for the 5 identified dopamine neurons that exhibited an excitation at the offset of the footshocks. (*E*) Higher-resolution population peristimulus time histograms (50-ms bins; mean) showing latency of the peak response at the offset of footshocks.

In conclusion, we show here that dopamine neurons located in the ventral VTA are excited by noxious footshocks, in contrast to dorsal VTA dopamine neurons, which are inhibited. We suggest that these 2 anatomically discrete populations represent 2 functionally distinct dopamine systems within the VTA.

Materials and Methods

Rats were treated in accordance with the Animals (Scientific Procedures) Act 1986 (United Kingdom).

Surgery. Sprague–Dawley rats (250–400 g; Charles River) were anesthetized with urethane (1.3 g/kg, i.p.; Sigma) plus supplemental doses of ketamine (20 mg/kg, i.p.; Ketaset; Willows Francis) and xylazine (2 mg/kg, i.p.; Rompun; Bayer) as required. Body temperature was maintained by using a homeothermic heating device (Harvard Apparatus). The depth of anesthesia was assessed by testing reflexes to a hind-paw pinch. Corneal dehydration was prevented with application of Lacri-lube eye ointment (Allergan Pharmaceuticals). A wide craniotomy was performed centered above the VTA (rostral-caudal: −5.3 mm from bregma) on either side of the sagittal suture. The prominent blood vessel on the sagittal sinus was heat-cauterized at the 2 ends (rostral and caudal) of the opening without damaging the underlying cortex and removed along with the dura from the exposed brain area. Saline solution (0.9% NaCl) was applied to the exposed cortex to prevent dehydration during recording.

Electrophysiology. Glass microelectrodes were lowered into the VTA by using a micromanipulator (LSS-8000 Inchworm Microdrive System; Burleigh) to a depth of 7.8–9.0 mm (rostral-caudal: 5.0–6.0 mm; medial-lateral: 0.3–1.0 mm). Extracellular neuronal activity was monitored by using the glass microelectrode [filled with 1.5% Neurobiotin; (Vector Laboratories) in 0.5 M NaCl], which was broken back to give a final tip diameter of 1–2 μm and a resistance of 6–15 MΩ (in situ). Extracellular recordings were AC-coupled, amplified ($\times$1,000), bandpass-filtered between 0.3 or 0.05 and 5 kHz (NeuroLog System; Digitimer), and acquired with Spike2 software (version 5.08; Cambridge Electronic Design) on a PC. Electrical interference from analog signals was minimized by using HumBug (Quest Scientific). The signals were then displayed on a digital oscilloscope (TDS 2002B; Tektronics) and captured by using a 1401plus A-D converter (Cambridge Electronic Design). Data were collected from neurons exhibiting broad APs with an initial positive deflection and a spontaneous firing rate $<$10 Hz. Spike2 software was used to analyze data offline. Neuronal activity was typically measured for 2 min each at 2 different filter settings (0.05–5 kHz and 0.3–5 kHz) before the onset of the noxious stimuli. Recordings from 0.3- to 5-kHz filter settings provided the baseline firing profile of individual neurons and their response to the experimental paradigm. Noxious stimuli were delivered via 2 silver wires (0.37-mm diameter), one attached to the plantar surface of the heel and the other to the ball of the little toe on the lateral side of the hind paws of the rats. Noxious electrical stimulations (3 trains in each series: 5 mA, 20 Hz, 4-s duration, 60-s intertrain interval) were administered by using CED 1401 computer interface and a constant current isolated stimulator (DS3; Digitimer) to hind paws. Initially, they were delivered on ipsilateral or contralateral sides of the VTA recording site. Because there were no significant differences in recordings between the 2 sides, for subsequent experiments 3 trains of multiple electrical stimulations were given only on the side contralateral to the VTA recording site and repeated after an interval of 60–120 s.

Juxtacellular Labeling. Following recording, neurons were selectively labeled by using the juxtacellular technique (14). Briefly, positive current pulses were applied through the microelectrode (200-ms duration, 50% duty cycle, 2.5 Hz, 1–20 nA). The amount of current applied was continuously monitored and adjusted to obtain modulation of AP activity in the neuron (i.e., increase in firing to passage of positive currents only). Modulation of firing was required to obtain detectable Neurobiotin labeling of the soma and dendrites of the recorded neuron.

Immunohistochemistry. At the end of the experimental session, animals were given a lethal dose of anesthetic then transcardially perfused with 200 mL of 0.1 M PBS solution at pH 7.4, followed by 400 mL of 4% paraformaldehyde (PFA) solution. The brain was subsequently removed and postfixed overnight in 4% PFA. Initially, coronal sections (60 μm) were made on a vibrating Microtome (VT1000S; Leica Microsystems) using PBS in the bath. Sections were incubated in a blocking solution [PBS with 10% normal goat serum (Jackson ImmunoResearch), 0.5% Triton X-100, and 1% BSA] for 1 h at room temperature, and then incubated for 72 h (4 °C) in mouse monoclonal antibody

NEUROSCIENCE

against TH (1:1,000; Sigma) in PBS with 2% normal goat serum, 0.5% Triton X-100, and 1% BSA to determine whether the neurons were dopaminergic. Following this, sections were rinsed several times in PBS and then incubated for a further 18–24 h (4 °C) in either Cy3-conjugated streptavidin and Cy5-conjugated donkey anti-mouse antibodies or Cy2-conjugated streptavidin and Cy3-conjugated donkey anti-mouse antibodies (1:1,000; Jackson ImmunoResearch) in PBS with 2% normal goat serum, 0.5% Triton X-100, and 1% BSA. Sections were then rinsed in PBS and mounted on slides in Vectashield (Vector Laboratories) for viewing under a fluorescence microscope (DM4000B; Leica Microsystems). After the initial experiments, we modified our protocol (as detailed below) to improve the penetration of the antibody, allowing inclusion of labeled neurons deep in the tissue which under the previous protocol would have been rejected from our analysis. After perfusion and fixation as described above, the whole rat brain was cryoprotected in 30% sucrose in PBS, embedded in OCT medium, frozen in isopentane at −50 °C, and sectioned at 30 μm on a cryostat (CM1800; Leica Microsystems). The floating sections were rinsed in PBS and then in 0.2% Triton-PBS solution or only in PBS. In the next stage, the sections were incubated in blocking solution (PBS with 6% normal donkey serum, 0.2% Triton X-100) for 1 h at room temperature and transferred into primary antibody solution of polyclonal rabbit antibody against TH (1:1,000 or 1:2,000; Calbiochem) in PBS with 2% normal donkey serum and 0.2% Triton X-100. Following overnight incubation at room temperature, sections were rinsed several times in PBS with 0.2% Triton X-100 and incubated for another 2–4 h at room temperature in secondary antibody solution consisting of Cy3- or Cy2-conjugated streptavidin (1:1,000; Jackson ImmunoResearch) and Alexa 488-conjugated goat anti-rabbit antibodies (Invitrogen) or Cy3-conjugated to donkey anti-rabbit antibodies Jackson ImmunoResearch [both 1:1,000; in PBS with 2% normal donkey serum, 0.2% Triton X-100]. Sections were rinsed in PBS with 0.2% Triton X-100 and then PBS solution only and mounted on slides and dried. Coverslips were placed on the slides after applying Vectashield or Gel Mount (Sigma) for visualization and identification. Images were stored digitally by using Leica FireCam software (version 1.7.1) on an Apple Mac G3.

Anatomical Localization of Labeled Neurons. Cytoarchitectonic features of the VTA and the surrounding areas and, more specifically, of TH-positive neurons, including their distribution (density) and their morphology (size, orientation, dendritic arborization), as described by Ikemoto (11), were used to precisely determine the anatomical localization of neurobiotin-labeled cells. These neurons were then plotted onto coronal figures from the rat brain atlas of Paxinos and Watson (16). This plotting was done blind to the physiology of the individual neurons. To more clearly depict dorsal and ventral differences, we made a single schematic sagittal view of the VTA (lateral 0.6 mm), on which we plotted all left and right side labeled neurons.

Data Analysis. Each trace was visually inspected to ensure that the spikes identified were distinct from the noise and other artifacts. The baseline firing rate of each neuron was quantified by averaging a 2-min recording session (with bandpass filter settings of 0.3–5 kHz) before the application of the noxious stimuli. For each neuron, an average spike waveform width was calculated from the recordings under the 2 filter settings described earlier. Width was determined as the time from the onset of the AP to the negative trough (6).

Statistical Analysis. Peristimulus time histograms using 500-ms bins were created from the average of firing rate obtained during all of the noxious stimulations. A neuron was considered responsive (excited or inhibited) if the mean firing rate during the first 500 ms following onset of the stimulus showed a change of 1.96 standard deviations from the mean baseline firing rate measured from the 10-s window before the onset of stimulation. Neurons that failed this criterion were considered to be unresponsive. Excitation at the termination of the noxious stimulation was determined for the first 500 ms following stimulation offset by using the same criterion (i.e., 1.96 standard deviations above the mean baseline firing rate). For each neuron, coefficient of variation of ISI was calculated as the ratio of the standard deviation to the mean of the ISI for the 2-min baseline recording session. Statistical comparisons of percentage of spikes in a burst and coefficient of variation of ISIs of excited versus inhibited dopamine neurons were made by using Mann–Whitney U tests with a significance level of $P < 0.05$. Statistical comparison of AP waveform widths and firing rates of different classes of recorded neurons were done by using a 2-tailed t test with a significance level of $P < 0.05$.

ACKNOWLEDGMENTS. We thank Matthew Bishop, Paul Bolam, Matthew Brown, Peter Dayan, Antonios Dougalis, Pablo Henny, Peter Magill, and Judith Schweimer for comments on this manuscript. This work was supported by U.K. Medical Research Council Grants U120085816 and G0400313 (to M.A.U.) and a University Research Fellowship from The Royal Society (to M.A.U.).

1. Schultz W (1998) Predictive reward signal of dopamine neurons. *J Neurophysiol* 80:1–27.
2. Wise RA (2004) Dopamine, learning and motivation. *Nat Rev Neurosci* 5:483–494.
3. Ford CP, Mark GP, Williams JT (2006) Properties and opioid inhibition of mesolimbic dopamine neurons vary according to target location. *J Neurosci* 26:2788–2797.
4. Lammel S, et al. (2008) Unique properties of mesoprefrontal neurons within a dual mesocorticolimbic dopamine system. *Neuron* 57:760–773.
5. Margolis EB, Mitchell JM, Ishikawa J, Hjelmstad GO, Fields HL (2008) Midbrain dopamine neurons: Projection target determines action potential duration and dopamine D2 receptor inhibition. *J Neurosci* 28:8908–8913.
6. Ungless MA, Magill PJ, Bolam JP (2004) Uniform inhibition of dopamine neurons in the ventral tegmental area by aversive stimuli. *Science* 303:2040–2042.
7. Abercrombie ED, Keefe KA, DiFrischia DA, Zigmond MJ (1989) Differential effect of stress on in vivo dopamine release in striatum, nucleus accumbens, and medial frontal cortex. *J Neurochem* 52:1655–1658.
8. Kalivas PW, Duffy P (1995) Selective activation of dopamine transmission in the shell of the nucleus accumbens by stress. *Brain Res* 675:325–328.
9. Pezze MA, Feldon J (2004) Mesolimbic dopaminergic pathways in fear conditioning. *Prog Neurobiol* 74:301–320.
10. Faure A, Reynolds SM, Richard JM, Berridge KC (2008) Mesolimbic dopamine in desire and dread: Enabling motivation to be generated by localized glutamate disruptions in nucleus accumbens. *J Neurosci* 28:7184–7192.
11. Ikemoto S (2007) Dopamine reward circuitry: Two projection systems from the ventral midbrain to the nucleus accumbens-olfactory tubercle complex. *Brain Res Rev* 56:27–78.
12. Hasue RH, Shammah-Lagnado SJ (2002) Origin of the dopaminergic innervation of the central extended amygdala and accumbens shell: A combined retrograde tracing and immunohistochemical study in the rat. *J Comp Neurol* 454:15–33.
13. Haber SN, Fudge JL, McFarland NR (2000) Striatonigrostriatal pathways in primates form an ascending spiral from the shell to the dorsolateral striatum. *J Neurosci* 20:2369–2382.
14. Pinault DA (1996) Novel single-cell staining procedure performed in vivo under electrophysiological control: Morpho-functional features of juxtacellularly labeled thalamic cells and other central neurons with biocytin or Neurobiotin. *J Neurosci Methods* 65:113–136.
15. Urch CE, Donovan-Rodriguez T, Dickenson AH (2003) Alterations in dorsal horn neurones in a rat model of cancer-induced bone pain. *Pain* 106:347–356.
16. Paxinos G, Watson C (2007) *The Rat Brain in Stereotaxic Coordinates* (Academic, Sydney), 6th Ed.
17. Grace AA, Floresco SB, Goto Y, Lodge DJ (2007) Regulation of firing of dopaminergic neurons and control of goal-directed behaviors. *Trends Neurosci* 30:220–227.
18. Steffensen SC, Svingos AL, Pickel VM, Henriksen SJ (1998) Electrophysiological characterization of GABAergic neurons in the ventral tegmental area. *J Neurosci* 18:8003–8015.
19. Luo AH, Georges FE, Aston-Jones GS (2008) Novel neurons in ventral tegmental area fire selectively during the active phase of the diurnal cycle. *Eur J Neurosci* 27:408–422.
20. Yamaguchi T, Sheen W, Morales M (2007) Glutamatergic neurons are present in the rat ventral tegmental area. *Eur J Neurosci* 25:106–118.
21. Nair-Roberts RG, et al. (2008) Stereological estimates of dopaminergic, GABAergic and glutamatergic neurons in the ventral tegmental area, substantia nigra and retrorubral field in the rat. *Neuroscience* 152:1024–1031.
22. Matsumoto M, Hikosaka O (2007) Lateral habenula as a source of negative reward signals in dopamine neurons. *Nature* 447:1111–1115.
23. Grace AA, Bunney BS (1984) The control of firing pattern in nigral dopamine neurons: burst firing. *J Neurosci* 4:2877–2890.
24. Gonon FG (1988) Nonlinear relationship between impulse flow and dopamine released by rat midbrain dopaminergic neurons as studied by in vivo electrochemistry. *Neuroscience* 24:19–28.
25. Overton PG, Clark D (1997) Burst firing in midbrain dopaminergic neurons. *Brain Res Rev* 25:312–334.
26. Tanimoto H, Heisenberg M, Gerber B (2004) Event timing turns punishment to reward. *Nature* 430:983.
27. Daw ND, Kakade S, Dayan P (2002) Opponent interactions between serotonin and dopamine. *Neural Netw* 15:603–616.
28. Coizet V, Dommett EJ, Redgrave P, Overton PG (2006) Nociceptive responses of midbrain dopaminergic neurones are modulated by the superior colliculus in the rat. *Neuroscience* 139:1479–1493.
29. Joseph MH, Datla K, Young AM (2003) The interpretation of the measurement of nucleus accumbens dopamine by in vivo dialysis: The kick, the craving or the cognition? *Neurosci Biobehav Rev* 27:527–541.
30. Moutoussis M, Bentall RP, Williams J, Dayan P (2008) A temporal difference account of avoidance learning. *Network* 19:137–160.
31. Ungless MA (2004) Dopamine: The salient issue. *Trends Neurosci* 27:702–706.
32. Horvitz JC (2000) Mesolimbocortical and nigrostriatal dopamine responses to salient non-reward events. *Neuroscience* 96:651–656.

33. Redgrave P, Prescott TJ, Gurney K (1999) Is the short-latency dopamine response too short to signal reward error? *Trends Neurosci* 22:146–151.
34. Carlezon WA, et al. (2000) Distinct sites of opiate reward and aversion within the midbrain identified using a herpes simplex virus vector expressing GluR1. *J Neurosci* 20:RC62.
35. Bolanos CA, et al. (2003) Phospholipase Cγ in distinct regions of the ventral tegmental area differentially modulates mood-related behaviors. *J Neurosci* 23:7569–7576.
36. Ikemoto S, Murphy JM, McBride WJ (1997) Self-infusion of $GABA_A$ antagonists directly into the ventral tegmental area and adjacent regions. *Behav Neurosci* 111:369–380.
37. Ikemoto S, Murphy JM, McBride WJ (1998) Regional differences within the rat ventral tegmental area for muscimol self-infusions. *Pharmacol Biochem Behav* 61:87–92.
38. Olson VG, et al. (2005) Regulation of drug reward by cAMP response element-binding protein: Evidence for two functionally distinct subregions of the ventral tegmental area. *J Neurosci* 25:5553–5562.
39. Fa M, et al. (2003) Electrophysiological and pharmacological characteristics of nigral dopaminergic neurons in the conscious, head-restrained rat. *Synapse* 48:1–9.
40. Hyland BI, Reynolds JN, Hay J, Perk CG, Miller R (2002) Firing modes of midbrain dopamine cells in the freely moving rat. *Neuroscience* 114:475–492.
41. Mirenowicz J, Schultz W (1996) Preferential activation of midbrain dopamine neurons by appetitive rather than aversive stimuli. *Nature* 379:449–451.
42. Schultz W, Romo R (1987) Responses of nigrostriatal dopamine neurons to high-intensity somatosensory stimulation in the anesthetized monkey. *J Neurophysiol* 57:201–217.